Earth and Planetary Science Letters 277 (2009) 355–364

Contents lists available at ScienceDirect

Earth and Planetary Science Letters

journal homepage: www.elsevier.com/locate/epsl

# Comparing crustal and mantle fabric from the North American craton using magnetics and seismic anisotropy

Götz H.R. Bokelmann [a,*], Andreas Wüstefeld [a,b]

[a] Université Montpellier II, CNRS, Laboratoire Géosciences Montpellier, Place Eugène Bataillon, CC060, 34095 Montpellier cedex 5, France
[b] Dept. of Earth Sciences, University of Bristol, Wills Memorial Building, Queen's Road, Bristol, BS8 1RJ, United Kingdom

ARTICLE INFO

*Article history:*
Received 22 July 2008
Received in revised form 27 October 2008
Accepted 29 October 2008
Available online 6 December 2008

Editor: R.D. van der Hilst

*Keywords:*
seismic anisotropy
shear-wave splitting
lithosphere
magnetics
fabrics

ABSTRACT

A central target in Earth sciences is the study of deformation at various depth levels within the Earth. Seismology has offered a remarkable tool for doing this via seismic anisotropy. It is however not always clear how to interpret those observations. A question of interest is to understand the relation between the deformation of the mantle and the crust, and in studying the relation between the two. Mantle deformation is expressed in seismic anisotropy. In this paper we seek an objective way of extracting information about crustal fabric as well, to be able to compare with seismic anisotropy. The magnetization of crustal rocks offers an attractive possibility for doing this. We thus explore the use of magnetic data, and we compare magnetic crustal fabric orientation with mantle fabric observations from seismic anisotropy. We apply our technique to the North American craton for which we have an excellent magnetic dataset, and we show that there is a clear relation between crustal and mantle fabric for the cratonic region. This has important implications for crustal formation, and for interpreting seismic anisotropy observations.



## 1. Introduction

The study of deformation within the Earth is a central interest of tectonics. As the gradient of displacement, deformation helps to unravel relative motion (current or ancient) recorded in the rock sequence, and it may also help to constrain stress. At the surface of the Earth, deformation is apparent in outcrops studied by field geologists, but there are only a few types of observations that constrain deformation within the Earth's interior. Xenolith studies offer a window on deformation at small-scales for rocks that are now at the surface and may or may not be typical for the mantle (Mainprice et al., 2000).

In the last decades, seismic anisotropy has offered an attractive way of studying deformation within the Earth (e.g., Silver et al., 1999). This allows us in principle to constrain deformation and motion within the deeper Earth, and especially, whether the motion of the crust and the mantle portion of the lithosphere is coherent, or whether there is relative motion between the two. The relation between deep deformation and surface tectonics has many important implications. One of the questions of interest in various tectonic environments is whether crust and mantle are 'coupled' (or decoupled), that is whether they are moving coherently or independently (e.g., Teyssier et al., 1995; Schulte-Pelkum et al., 2001; Bokelmann and Silver, 2002; Tikoff et al., 2004). This is important for better understanding mantle rheology, and it may also serve to understand the role of the various forces driving the motion of lithospheric plates (e.g., Bokelmann, 2002a,b).

The present paper is focused on the origin of lithospheric roots, for which one of the guiding models is the "Vertically Coherent Deformation" model of Silver and Chan (1988, 1991), which suggests a similar deformation in crust and mantle lithosphere based on the coherence of observed mantle deformation with crustal deformation determined in the field by inspecting geological structures. However, concern has been raised by some (e.g., Vinnik et al., pers.comm.) about the subjective fashion that is employed in extracting crustal fabric features.

We will take up this comparison and present an objective way for extracting crustal fabric features, based on quantitative geophysical information. Our technique extracts preferred orientation information from potential field data, and more generally all kinds of mapped data. We will here focus on the crustal magnetic field. Magnetic data are particularly well-suited for our purpose, since smaller-scale features of the magnetic field at the Earth's surface (except for the long-wavelength core field) depend exclusively on the uppermost portion of the lithosphere, due to a limiting temperature for ferromagnetic behaviour, the Curie temperature. Magnetic data are available with high resolution. We will study the relation between seismic anisotropy and crustal magnetic fabric for North America. A first inspection has shown similarities between linear structures present in the magnetic maps and the shear-wave splitting fast directions. This has attracted our attention, and we present here an objective comparison using a Radon Transform to extract dominant orientations in the magnetic field data. Our primary goal is to understand the deformation of the upper mantle

* Corresponding author. Tel.: +33 4 67 14 33 49; fax: +33 4 67 14 36 03.
*E-mail address:* Goetz.Bokelmann@gm.univ-montp2.fr (G.H.R. Bokelmann).

0012-821X/$ – see front matter © 2008 Elsevier B.V. All rights reserved.
doi:10.1016/j.epsl.2008.10.032

and especially the origin of the deep lithospheric keels under the cratons, e.g., whether these have been created at the same time as the ancient crust, or more recently.

## 2. Preferred orientations in the mantle from seismic anisotropy

Deformation in the Earth can be constrained by seismic anisotropy, since the latter is caused by deformation-induced alignment of anisotropic minerals, and especially olivine, into "crystal-preferred-orientations" (CPO) (Nicolas and Christensen, 1987). A deformation event may erase any existing CPO relatively quickly by developing new fabric or by recrystallization processes (Nicolas et al., 1973; Mainprice and Silver, 1993). Therefore, any anisotropy can be assumed to reflect the last period of significant deformation, or the last thermal event. In stable tectonic regimes, the anisotropy caused by the last period of deformation may remain "frozen" in the lithospheric rocks during post-tectonic thermal relaxation (Vauchez and Nicolas, 1991; James and Assumpcao, 1996; Barruol et al., 1997; Barruol et al., 1998; Heintz and Kennett, 2006).

The effect of seismic anisotropy is present in all kinds of seismic waves: Surface waves (e.g., Montagner, 1986), P- and Pn-wave delays (e.g., Raitt et al., 1969; Babuška et al., 1984; Babuska and Cara, 1991; Bokelmann, 2002a; Schulte-Pelkum and Blackman, 2003), P-wave polarization (Bokelmann, 1995; Schulte-Pelkum et al., 2001), and particularly in shear-waves via shear-wave splitting (Fukao, 1984; for reviews see Silver, 1996 and Savage, 1999). The different techniques provide very different constraints on seismic anisotropy. Pn-waves provide very good vertical resolution (just below the Moho), as do, to slightly lesser degree, surface waves. Both types of constraints average laterally over hundreds to thousands of kilometers, and their usefulness for studying structures within cratons is thus limited, since the latter may well vary significantly over those length scales. The best-suited technique for addressing the questions raised above is in fact shear-wave splitting, since it provides excellent lateral resolution, at the price of weak vertical resolution within the upper mantle.

A teleseismic S-wave refracting at the Earth's core is polarized within the sagittal plane. Impinging on an anisotropic medium, it splits into two components. This phenomenon is called seismic birefringence or shear-wave splitting. The two components are polarized in mutually perpendicular directions, and they travel at different speeds. The time delay d$t$ between the two S phases, arriving at the surface as well as the polarization direction $\Phi$ of the faster S wave serve as measures of the anisotropy in the subsurface. These two parameters can be extracted efficiently, e.g., using computer codes that we have made available to researchers in the field recently (e.g., Wüstefeld et al., 2008).

The technique of shear-wave splitting has been widely applied in many regions around the Earth, and it has shown its great utility for deciphering deep deformation in various settings of active tectonics (e.g., Wüstefeld et al., submitted for publication). In contrast to those active zones, cratons constitute the old, stable parts of continents that have not shown tectonic activity for a long time. There are only a limited number of shear-wave splitting studies in such areas (Canadian shield, Kaapvall craton, Baltic Shield, Australian shield, and others; see Fouch and Rondenay, 2006 for a review). The information on upper mantle deformation that they supply is particularly valuable for cratonic regions, where other observational constraints on deep deformation, such as lithospheric flexure, are lacking. Cratonic regions are generally associated with thick lithospheric roots that apparently move coherently with the plates. This raises the question of how and where the relative motion between surface plate and deeper mantle is taking place. Perhaps thick lithospheric roots act as keels that deviate mantle flow around them (McKenzie, 1979; Bormann et al., 1993, Fouch et al., 2000). Seismic anisotropy in such environments may help to distinguish present day deformation at depth, associated with plate motion (McKenzie, 1979), from fossil deformation (Bokelmann, 2002a,b; Bokelmann and Silver, 2000).

Since the first applications of shear-wave splitting (Ando and Ishikawa, 1982; Vinnik et al., 1984; Fukao, 1984; Bowman and Ando, 1987; Silver and Chan, 1988; Ansel and Nataf, 1989) numerous studies have been performed. North America has been relatively well sampled (see references in Fouch and Rondenay, 2006). Fig. 1a shows shear-wave splitting measurements on the North American Craton. These are taken from the shear-wave splitting database (Wüstefeld et al., submitted for publication, http://www.gm.univ-montp2.fr/splitting/DB), originating from studies by Silver and Chan (1988, 1991), Vinnik et al. (1992); Silver and Kaneshima (1993); Sénéchal et al. (1996); Ji et al. (1996); Barruol et al. (1997), Kay et al. (1999); Bank et al. (2000); Rondenay et al. (2000a,b); Snyder et al. (2003); Eaton et al. (2004). The data set is representative for the North American craton, although some of the more recent experiments may perhaps not yet be included, e.g., recent studies using Polaris data.

In this study, we focus on stations on or near the Precambrian portion of the crust in the central northern part of North America. This portion corresponds closely to the part of the continent that is associated with high average velocities in the upper mantle, shown by the thick line in Fig. 1a (from Bokelmann, 2002b) outlining regions more than 0.2 km/s faster than the global average in the tomographic

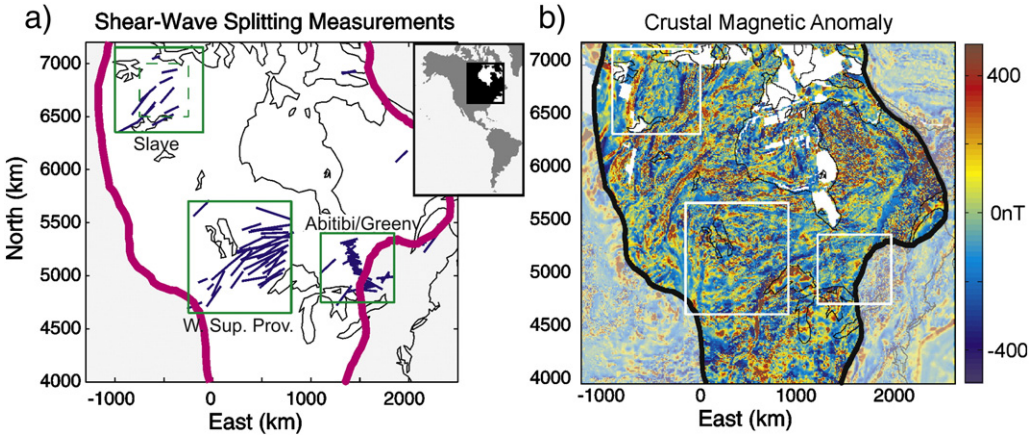


**Fig. 1.** a) Shear-wave splitting measurements (non-Nulls) for the North American craton. For each measurement, the orientation of the (blue) line gives the fast direction, and the length gives the splitting delay d$t$ (see text). Rectangles give regions of particular interest that will be studied in more detail below. b) Magnetic map for North America (in nanoTesla; after Bankey et al., 2002). The map is truncated at −500 and 500 nT (nanoTesla) to emphasize linear features. See text for more details. (For interpretation of the references to colour in this figure legend, the reader is referred to the web version of this article.)

model of Grand (1994). A fast mantle indicates the presence of a thick lithosphere under the old cratonic crust. The anisotropy at each station is characterized by a fast direction $\Phi$ and a splitting delay d$t$ that is up to a maximum value of 2.15 s at station SAO (lat. 36.765N, long. 121.445W). We focus on stations within or near that portion, north of 45° latitude where Precambrian rocks outcrop at the surface. For the few stations that show two layers of anisotropy, in the sense of Silver and Savage (1994), we use the shallower one.

The crust is known to contribute only a few tenths of a second to the total splitting (Barruol and Mainprice, 1993). The crust can therefore explain only a small portion of the observed splitting particularly in this area of high d$t$, which we have confirmed by numerical modeling experiments. This modeling has also shown that the crustal anisotropy has only minor effect on the observed fast directions. Most of the observed shear-wave splitting is apparently due to the upper mantle; potential deeper anisotropy has a strong effect on the observations made at the surface only if it is coherent over the entire lateral Fresnel zone that is much wider at those depths (e.g., Sieminski et al., 2007).

Fig. 1b shows magnetic field anomalies at the Earth's surface (after Bankey et al., 2002) which we will discuss in detail below. Comparing alignment directions of magnetic lineaments visually with seismic fast directions, we have noted a certain correlation. This has motivated the present study.

## 3. Magnetic properties of the lithosphere

Crustal and lithospheric magnetic properties are dominated by the ingredients of ferro- or ferri-magnetic minerals in the bulk rock. The most magnetic of these minerals is magnetite ($Fe_3O_4$), which is furthermore present in considerable quantities throughout the lithosphere. Magnetite is a ferrimagnetic mineral with very strong susceptibility. Beyond its characteristic Curie temperature of about 580 °C, magnetite loses its ferrimagnetism. The magnetism is then dramatically weaker, and controlled only by paramagnetism. The Curie temperature is found to increase with pressure by about 20 K/GPa (Samara and Giardini, 1969; Schult, 1970). Fig. 2 shows geothermal profiles typical for both hot and cold lithosphere (after Karato and Wu, 1993). These profiles intersect with the Curie temperature in the upper lithosphere, at depths not far from the crust–mantle boundary. This suggests that magnetization is weak in deeper portions of the lithosphere, in particular the depth region which corresponds to the observed seismic anisotropy. Maximum depths of ferrimagnetic behavior in the Earth correspond roughly to the depth obtained independently using spectral analysis of magnetic data at the surface (e.g., Chiozzi et al., 2005).

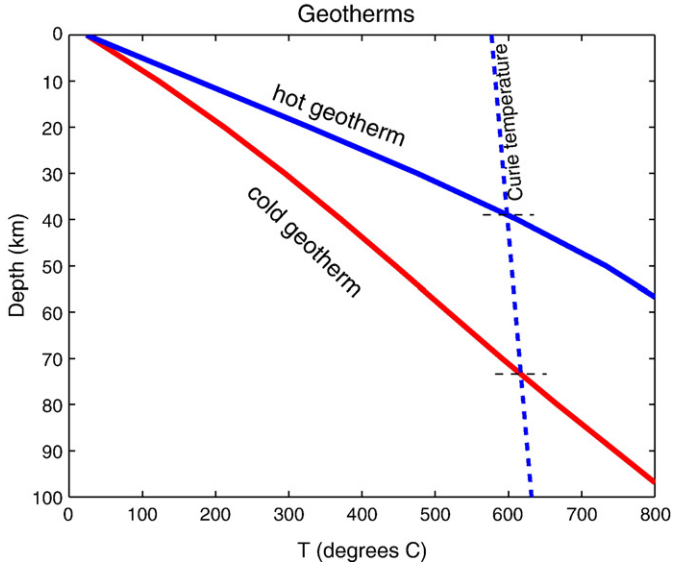


**Fig. 2.** Curie temperature for geothermal profiles corresponding to a hot (tectonic) lithosphere and a cold (cratonic) lithosphere (see text). The dashed line shows the slight pressure-dependence of the Curie temperature.

Magnetic anomalies are thus sensitive essentially exclusively to the Earth's crust. Short-wavelength magnetic lineaments therefore provide a way to study crustal fabric that can then be compared with mantle fabric from seismic anisotropy. Beside the depth distribution of the magnetization, the distance from the surface also plays a role since the magnetic field decays strongly ($\sim r^{-3}$) with distance. It is thus clear that the magnetic field is influenced less by structures in the deep crust, even if there exist enhancement effects such as those described by Gilder et al. (2002).

## 4. Preferred directions in the crust from magnetics

This paper addresses the spatial patterns of magnetic field anomalies over Precambrian North America. Fig. 1b shows the high-resolution dataset for North America from Bankey et al. (2002), presented on a 1×1 km grid. Note that the spatial resolution is not the same everywhere, as high-resolution data are not available for all regions, e.g. for the Northern Rocky Mountain area and certain offshore areas. Regions of North America where no magnetic data are available are shown in white. This dataset has been assembled from aeromagnetic and satellite data and is downward-continued to a height of 300 m (1000 ft) above the surface. Aeromagnetic data provide high spatial resolution down to wavelengths of a few kilometers, while satellite data offer reliable long-wavelength information of up to 500 km. This long-wavelength limit excludes the strong core field. The (total intensity) magnetic anomalies regarded here are on the order of several hundreds of nanoTesla (nT). The data processing involved downward continuation (equivalent source method) of CHAMP data (Maus et al., 2002). The sequence of steps is described in Bankey et al. (2002).

Fig. 1b shows a fascinating array of magnetic structures, with positive and negative bands of various widths which vary smoothly in space. This smooth spatial variation is especially apparent for the craton, where bands are up to several thousand kilometers long. Off the craton, the appearance of the magnetic pattern is more diffuse, with apparently a lower degree of spatial organization. Inspecting images such as Fig. 1b visually, does however not necessarily reveal all magnetic structures: On one hand, there is potential variation at smaller scale lengths not visible in the map; on the other hand, variations at weaker (or stronger) level might be concealed by the color map. This is yet another reason for choosing an objective technique for characterizing the magnetic field.

We are looking for preferred orientations in the magnetic data $f(x,y)$. The natural way for doing this is to use a linear Radon transform

$$F(\theta, s) = \iint f(x, y)\delta(x\cos\theta + y\sin\theta - s)\mathrm{d}x\mathrm{d}y \quad (1)$$

to transform the magnetic field data $f(x, y)$, as has been done in other recent approaches (Zhang et al., 2006; Hansen and de Ridder, 2006). This transformation corresponds to a 'slant stack' along each direction $\theta$ (see Fig. 3). This procedure maps a linear feature in $f(x, y)$ into a point in $F(\theta,s)$ at slope angle $\theta$ and offset $s$. Furthermore, a point maps into a sinusoid in $F(\theta,s)$. The Radon transformation gives thus a basis for either detecting individual lineaments in the map, or for characterizing preferred orientation by summing over all offsets s in a suitable way. We are primarily interested in the overall preferred orientation ('alignment') rather than individual lineaments, and also in lineaments with both positive and negative amplitude. For this purpose we will in the following use the simple measure

$$P(\theta) = \int |F(\theta, s)|^p \mathrm{d}s / \max\left\{\int |F(\theta, s)|^p \mathrm{d}s\right\} \quad (2)$$

as proxy for the degree of alignment (DOA). The exponent p may be chosen larger than 1 to enhance the effect of linear features. We will

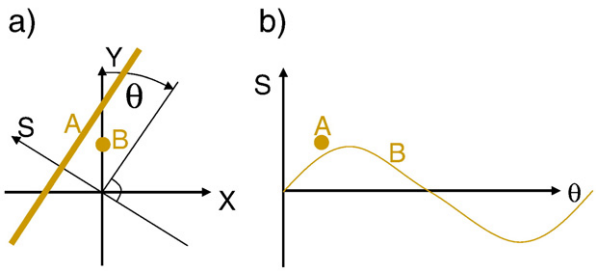


**Fig. 3.** Illustration of the Radon transformation: data $f(x,y)$ shown in a) map into $F(\theta,s)$ in b). As an example, a linear structure (A) is mapped into a point; a point is mapped into a sinusoid with an amplitude proportional to the distance of the point B to the origin of the geographical map.

use a value of $p=2$ in this study. As an alternative to the exponent, one might use semblance-based measures (e.g., Neidell and Taner, 1971) to increase the sensitivity. We also remove outliers in the magnetic map $f(x,y)$, that have absolute values of more than 5000 nT. This threshold is quite conservative, since the procedure is hardly sensitive to the presence of outliers.

Fig. 4 shows the processing sequence for example station RSON at Redlake, Ontario (latitude 50.86N, longitude 93.70W). a) shows the magnetic map around the station (in a spherical transverse Mercator projection). Note the linear features with positive/negative amplitudes (red/blue) with wavelength of 10 to 40 km that have a nearly East–West trend. We calculate Eqs. (1) and (2) for several circular regions around the station, with radii between 25 to 50 km. The largest circle size is made to roughly correspond to the Fresnel zone in the topmost upper mantle experienced by the shear waves with dominant period of 10 s, so that we compare the same regions in crust (magnetics) and mantle (seismic anisotropy). The variation of preferred orientation with search region will help to determine robustness of results and their statistical variation.

The Radon transform $F(\theta,s)$ in Fig. 4b (calculated for the largest circle) shows strong amplitudes, both positive and negative, indeed for angles $\theta$ between 500° and 100°. In addition, there are apparently points with strong amplitude in a) that map into a number of sinusoids in $F(\theta,s)$. The white line shows the normalized polarization $P(\theta)$. Fig. 4c) shows polar plots of (smoothed) $P(\theta)$, that have maxima ('preferred orientation') at approximately 80° for all circle sizes.

The procedure recovers preferred orientations that we would also have selected visually. The advantage of this technique is that it is reproducible and also objective in the sense that it depends on subjective criteria only through a set of parameters, most of which are in fact based on physical criteria (e.g., size of Fresnel Zone). Beside these, we require that data gaps constitute at most 5% of the circular test area, and we retain a preferred orientation only if there is clear alignment, that is $\min\{P(\theta)\}/\max\{P(\theta)\}$ needs to be smaller than 0.6.

The extracted magnetic orientation shown by the dashed line in Fig. 4a) agrees well with the fast direction from shear-wave splitting. The median magnetic direction is 75°, versus a seismic fast direction of 76°. We will see below however that there can be multiple sets of preferred alignment at a given station. A direct comparison of the two directions can therefore be misleading. An appropriate way to judge the agreement is to inspect the normalized degree of alignment

$$P_s(\theta) = \frac{P(\theta) - \min\{P(\theta)\}}{1 - \min\{P(\theta)\}}, \tag{3}$$

and to determine the quantile of the normalized magnetic alignment $P_s(\theta)$ that corresponds to the orientation of the seismic fast direction

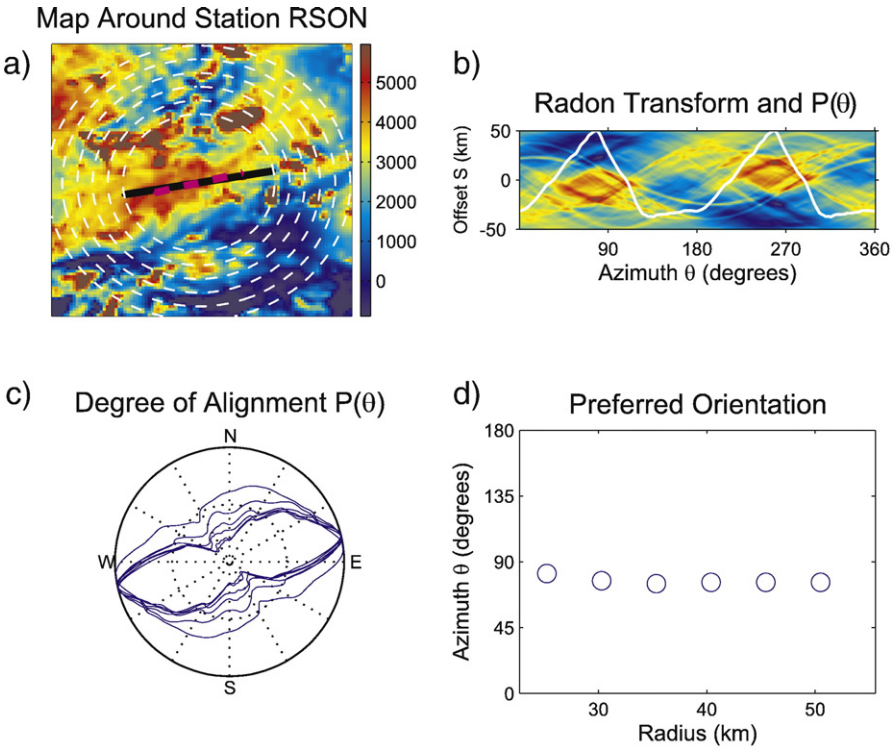


**Fig. 4.** Crustal and mantle structures for station Red Lake, Ontario: a) magnetic anomaly map $f(x,y)$ (100×100 km) around the seismological station RSON (latitude 50.86N, longitude 93.70W). The dashed magenta line shows the determined preferred direction from magnetics (crustal fabric); the solid black line shows the fast direction from SKS splitting (mantle fabric), with six different circular test regions (dashed white circles). The length shows the splitting delay (dashed magenta line gives a 1 second reference). b) shows the Radon transform of a) for the largest test region (as the colored background), together with the (normalized) degree of alignment $P(\theta)$ (as a white line). Red colors in b) indicate positive and blue colors negative values. c) shows a rose diagram with $P(\theta)$ for the six test regions from a); d) shows the preferred orientation as a function of radius, determined from a smoothed version of c). (For interpretation of the references to colour in this figure legend, the reader is referred to the web version of this article.)

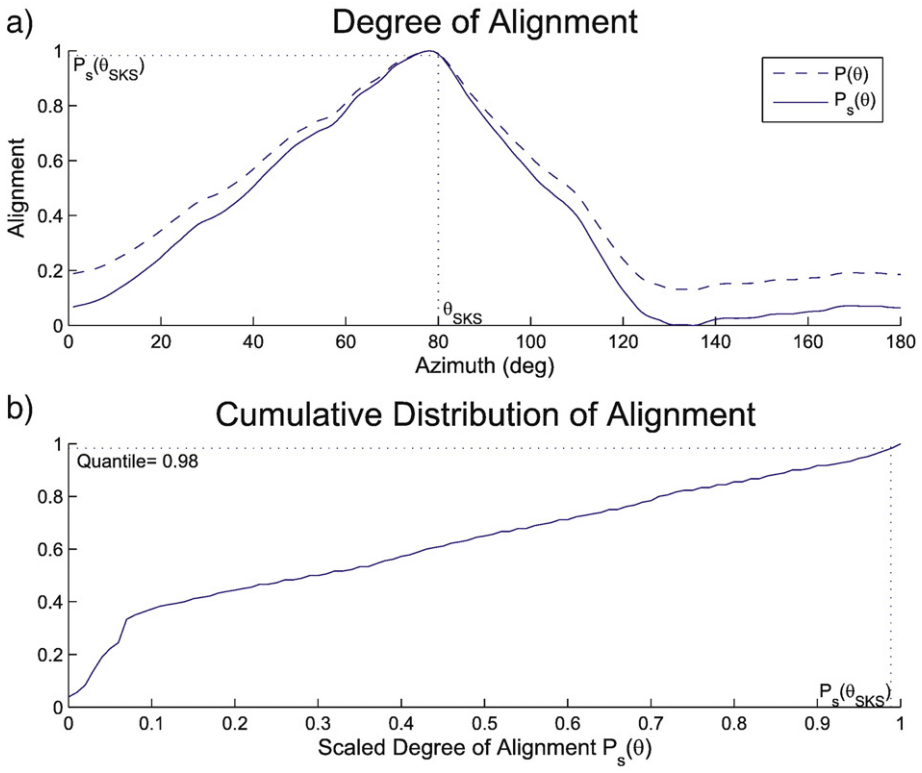


**Fig. 5.** Degree of alignment as a function of azimuth for the example station RSON as in Fig. 4 (shown between 0° and 180°). a) The degree of alignment $P(\theta)$ is shown by a dashed line, and the normalized DOA $P_s(\theta)$ by a solid line, together with the value corresponding to $\theta_{seis}$. b) shows the cumulative distribution of $P_s(\theta)$, and the determination of quantile values for $\theta_{seis}$. For station RSON, the quantile value is 0.98, indicating an excellent agreement. (see text).

$\theta_{seis}$ that is observed by shear-wave splitting. The quantile is defined as the fraction (or percent) of points below the given value. For example, we have a quantile of 0.9 (or 90%) if 90% of the total angular range (0° to 360°) is associated with magnetic alignments $P_s(\theta)$ that are weaker than the alignments corresponding to the seismic fast direction $P_s(\theta_{seis})$. In that case, the other 10% of the 360° angular range would show a better agreement than the direction corresponding to the seismic fast direction. The range of the quantile is between 0 and 1, with a value of 1 indicating the best possible agreement. A comparison of random orientations would, on the average, give a value of 0.5. Fig. 5 illustrates this procedure for the example from Fig. 4. For station RSON, the quantile is 0.98 (98%) which indicates an excellent agreement between seismic and magnetic orientations.

## 5. Application to the North American Craton

### 5.1. Superior Province

Fig. 4 has shown the application to a station in the Western Superior Province, RSON at Red Lake, Ontario. There are in fact three studies of seismic anisotropy at this station in the literature (Silver and Chan, 1991; Vinnik et al., 1992; Silver and Kaneshima, 1993) who obtained nearly the same results for the fast direction $\theta_{seis}$ = 76°/80°/76°, and identical values for d$t$ (1.7 s). The quantile values are 1.0/0.98/1.0.

Fig. 6 shows the Western Superior Province, giving available shear-wave splitting measurements (from Silver and Chan, 1988; Silver and Kaneshima, 1993; Kay et al., 1999) and the magnetic map. Fast

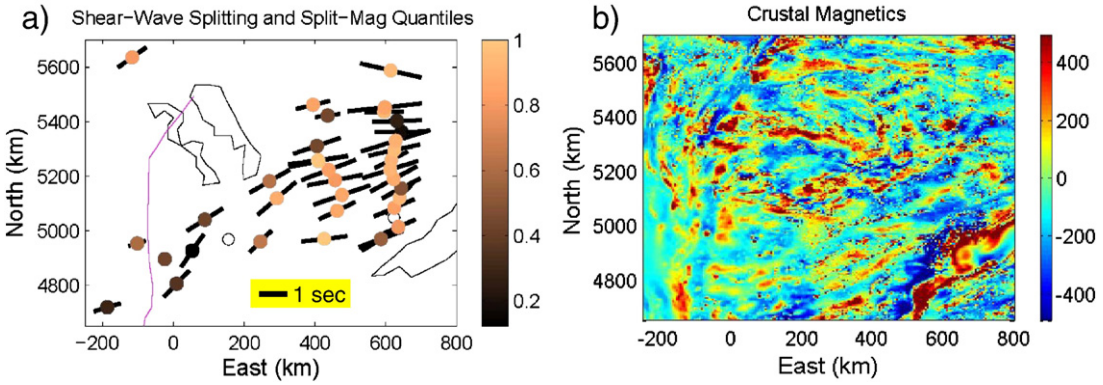


**Fig. 6.** The western Superior Province around station RSON (central panel of Fig. 1a). a) Lines show splitting measurements and colors/shading give quantile values for the comparison with the magnetic map in b). High quantile values (light shading) indicate good agreement. Note the generally very good agreement between fast directions and magnetic lineaments that is also apparent by visually comparing a) and b). The magenta line in a) gives the approximate location of the Superior Province – Trans-Hudson boundary (under sediments). Empty circles show stations where the magnetic alignment is not sufficiently strong. Magnetic data in b) are given in nT.

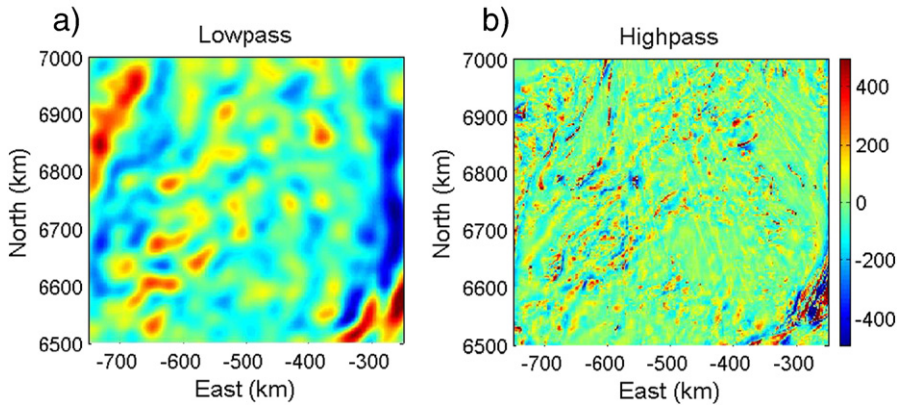


**Fig. 7.** Magnetic map for the Slave Craton (smaller panel in the northwest in Fig. 1a; given in nT). a) lowpass-filtered with $\lambda_{min}$ = 20 km. b) highpass-filtered at $\lambda_{max}$ = 20 km (see text).

orientations are mostly WSW–ENE in the Western Superior Province, e.g., near and to the south of station Red Lake which is in the center of the map. The magnetic map shows lineaments that visually agree more or less with the splitting orientations, especially for the central portion. This is corroborated by the very high quantile values (shown in a) at those stations. Both magnetic preferred orientation and seismic fast directions, agree well with the dominant feature directions in the Western Superior Province (e.g., Hoffman, 1989), and they show simultaneous rotation with them, such as the clockwise rotation in the northern part of the TWT transect (Kay et al., 1999). The agreement degrades somewhat for the stations further to the West. The five stations in the Southwest are on the Superior Province – Trans-Hudson boundary or already within the Trans-Hudson. Magnetic preferred directions for the Trans-Hudson orogen are in fact more or less North–South, which is in agreement with the dominant tectonic structures. Seismic fast directions at the SW stations are somewhat intermediate between these 'Trans-Hudson directions' and the WSW–ENE trend observed in the Western Superior Province. Nevertheless, 24 of the 38 stations have quantile values above 0.75, indicating that many of the stations in this region show a very good agreement between the two sets of orientations. The basement is covered by sediments of the Williston basin.

### 5.2. Slave Craton

We will now focus on the subregion indicated in the northwest of Fig. 1a, the Slave Craton. Seismic fast directions are mostly SW–NE for that region (Bank et al., 2000). We show the magnetic field for the central Slave craton (corresponding to the smaller window in Fig. 1a) in Fig. 7 a) and b), as low- and high-pass filtered images, selecting respectively either longer or shorter wavelengths than 20 km. The seismic directions agree more or less with lineations that are apparent in the lowpass-filtered magnetic map in a). On the other hand, wavelengths shorter than 20 km make a set of North–South trending lineaments appear (Fig. 7b). The presence of this secondary set of lineaments has in fact motivated the more elaborate statistical technique presented above.

The North–South trending lineaments are caused by dykes. These dykes are part of the massive MacKenzie dyke swarm, which radiates from a plume center west of Victoria Island (Ernst et al., 2001). Typical widths of these dykes are 20–50 m, and several of them are thousands of kilometers long (LeCheminant, 1994). The orientations of the dykes vary smoothly in space. The magnetic signal of the dykes becomes quite apparent in the highpass-filtered map. Their effects are still present in the low-pass filtered version though. This is seen for individual stations on the Slave craton. An alternative approach is to filter out the dyke signal using directional filtering, via a coordinate transformation approach (Pilkington and Roest (1998). For our study, we have decided to use the full information content of the original data, and to apply the statistical technique based on quantiles described above rather than comparing a preferred magnetic alignment with seismic fast directions. In the presence of dykes, quantile values for the comparison may be slightly underestimated.

Application of the code to individual stations has made the presence of these two sets of lineaments apparent for many stations on the Slave craton. The code finds two sets of preferred directions, one nearly East–West and one nearly North–South. For some stations, the North–South trending dykes produce a stronger magnetic lineament signature than the East–West trending lineaments.

Fig. 8a shows splitting data for the Slave Craton, which trend mostly in SW–NE direction along the craton. Quantile values show reasonable agreement between seismic and magnetic directions, despite the interference from the dykes. 4 stations out of 11 for which the analysis could be made, have quantile values of more than 0.75. The splitting directions (Bank et al., 2000) are in good agreement with fast directions from surface waves (e.g., Fouch and Rondenay, 2006), and they also agree with high-conductivity directions of around 80° from magnetotellurics (e.g., Eaton et al., 2004).

### 5.3. Abitibi/Grenville region

Fig. 8b shows a comparison for the third region indicated in Fig. 1a, the Abitibi/Grenville region. The Grenville Front separates the Archean Superior Province, named Abitibi in that region, from the Grenville Province. The latter consists of Proterozoic and reworked Archean rocks.

Mantle anisotropy in this region has been studied using seismology (Sénéchal et al., 1996; Ji et al., 1996; Fouch and Rondenay 1996; Rondenay et al., 2000a,b), and also using magnetotellurics. Shear-wave splitting is noticeably weaker than in the other two regions, with a mean of 0.7 s, as opposed to 1.3 s for the Western Superior Province and 1 s for the Slave Craton. This is perhaps due to its location closer to the edge of the shield, as is indicated from the +0.2 km/second line in Fig. 1a that passes close-by. A correlation of splitting delay times with upper mantle delay has previously been noted by Silver and Chan (1991), and it has been used to argue for a lithospheric origin of the observed anisotropy.

The correlation between fast directions and magnetic lineaments is quite good for the Abitibi, and also for stations further into the Grenville, but it is low for stations in the immediate vicinity of the Grenville front, that is stations on the Pontiac terrane, but also just south of the Grenville front. High-conductivity directions from magnetotellurics can be slightly different from the seismic fast directions, e.g., Ji et al. (1996) have suggested that the rotation of about 20° may indicate a dextral

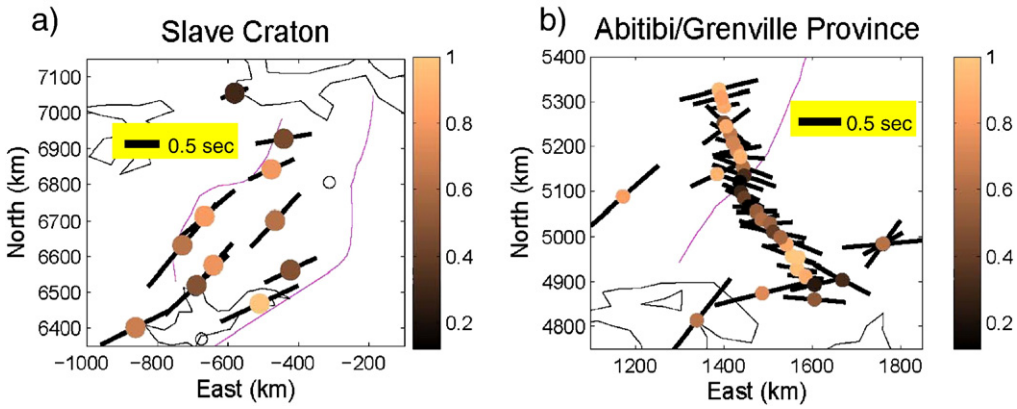


**Fig. 8.** Splitting fast directions (solid lines) and comparison with magnetic lineaments for a) the Slave Craton, and b) the Abitibi/Grenville region. The two regions are shown in Fig. 1a. Empty circles show stations where the magnetic alignment is not sufficiently strong. For better visualization, the splitting lines are shown twice as long as in Fig. 6.

shearing. This does however not appear to be a systematic feature in the region (Frederiksen et al., 2006).

## 6. Discussion

We have presented a technique for extracting lineament orientations from magnetic (and other map) data, and we have applied that technique to magnetic data from North America. Magnetic data are in principle ideally suited for extracting information on crustal fabric. For the Northern part of the North American craton, e.g. the Slave craton, these data are however, strongly influenced by magnetic perturbations from dykes. We have chosen an approach based on quantiles that is relatively insensitive to such interference.

We have seen that crustal magnetic fabric and seismic mantle anisotropy correlate well for different portions of the North American Craton. Fig. 9a shows a histogram of angular deviations between seismic fast axes and the preferred magnetic alignment (for the stations on the craton). The distribution is slightly off-center by −10°, and the standard deviation is relatively large ($\sigma$=40°), and somewhat better for the stations where splitting is stronger than d$t$>1.4 s (off-center by −7°, $\sigma$=32°). It is however clear that there is a correlation. As we have discussed above, a better representation in the presence of multiple sets of alignments is to inspect quantile values. Note that this distribution (Fig. 9b) clearly deviates from a random (uniform) distribution. This is especially the case for the set of stations where splitting is stronger than d$t$>1.4 s. We have inspected formal errors of

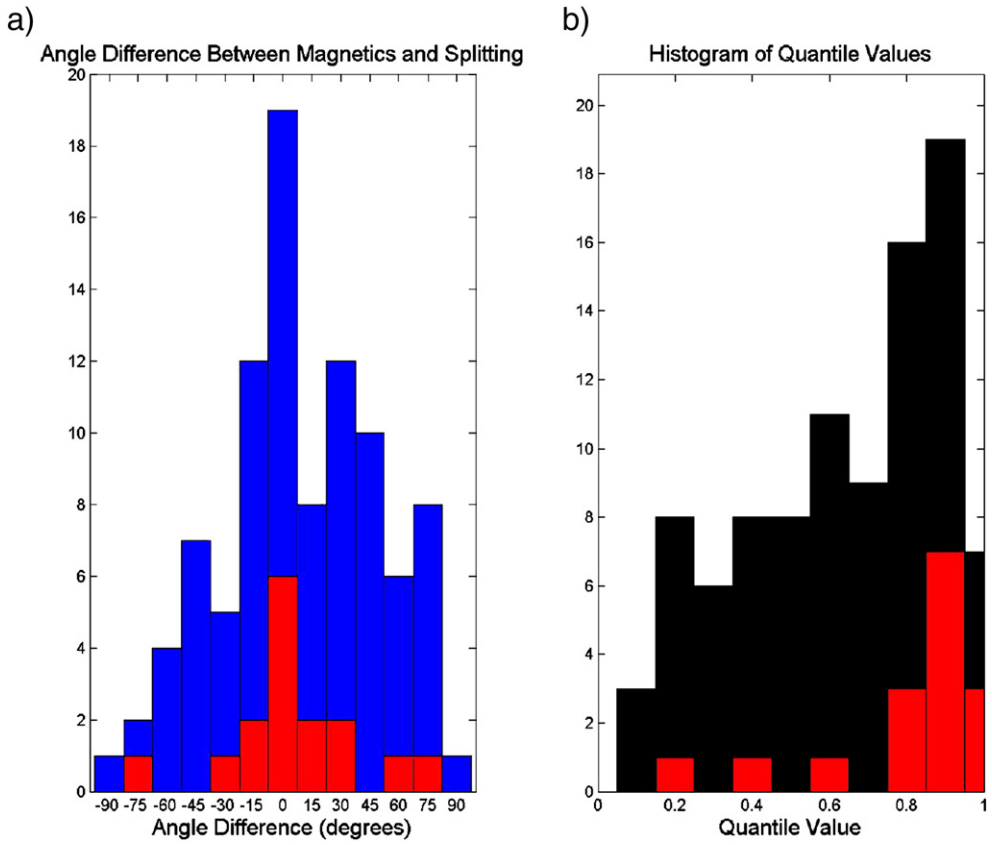


**Fig. 9.** Comparison of splitting fast directions and magnetic lineament directions. a) angular differences for all stations in Fig. 1, between magnetic preferred directions and seismic fast axes. b) histogram of quantile values for all stations. Red colors show the same for the smaller set of stations that have d$t$>1.4 s (see text). (For interpretation of the references to colour in this figure legend, the reader is referred to the web version of this article.)

$\theta_{seis}$ to test whether this may be due to the $\theta_{seis}$ being better determined than at other stations, and we find that this does not explain the stronger correlation by itself. The correlation is thus indeed better where splitting is stronger. The main results of the comparison are therefore:

1) There is a good correlation between crustal lineaments with mantle seismic fast directions,
2) This correlation is best where splitting is the strongest, and where the lithosphere is the thickest.

All this is especially the case in the Western Superior Province, where the lithosphere has not been significantly overprinted since the Archean. The correlation is somewhat weaker in the other zones we considered, the Trans-Hudson orogen, the Slave craton, and the Abitibi-Grenville region.

The Superior Province consists of East–West trending belts (Card, 1990), and they appear to have been assembled progressively from North to South. This suggests that the deformation associated with the collision of these belts was to large degree transpressive. Such a transpressive regime reorients all structures perpendicular to the compression direction. Magnetic lineaments appear to record that deformation reliably. This alignment is rather impressive in the Western Superior Province where magnetic lineaments are clearly closely parallel to the ancient suture zones (Hoffman, 1989, Card, 1990; Hoffman, 1990). We have also seen a second type of deformation (minor extension associated with dykes). Such dyke sets pervade much of the northern portion of the craton. These dykes clearly show up in the magnetic field, in addition to the effect of (older) crustal fabric (Fig. 7). There is no correlation of dyke orientations with seismic fast orientations. This suggests that the deformation associated with the dykes has not reset lithospheric fabric at scale lengths of our seismic waves (~100 km).

On the other hand, there is a robust correlation between seismic (mantle) anisotropy and (crustal) magnetic fabric. That robust correlation between crustal and mantle fabric gives us important clues on the processes that have formed the mantle lithosphere. The crust in some parts of the Canadian shields (Superior and Slave cratons) has not been significantly overprinted tectonically for at least 2.5 billion yrs. The similarity with the mantle suggests that the same is true for the mantle portion of the lithosphere as well.

The most natural explanation for the good correlation between crustal and mantle fabric is to suggest that the two depth layers were formed together, as is implied in a number of models for cratonic formation (e.g., Jordan, 1975, 1978, 1988; Silver and Chan, 1988; 1991). This would suggest that the mantle portion of the lithosphere was thus also created at least 2.5 billion yrs ago, together with the crust. The correlation is clearest for the Western Superior Province, which is a model region for Archean terranes, due to its large amount of unreworked Archean lithosphere. Fig. 10 shows a conceptual model for orientation of seismic fast directions, motivated by the vertically coherent deformation as described by Silver (1996). A lithosphere deforming by transpression produces a preferred orientation that is perpendicular to the compression direction. In the crust this alignment would manifest itself, amongst other, in an alignment of magnetic features. In the mantle, the same process produces an alignment of mineral grains, and especially olivine that would attain a preferred orientation of a-axes perpendicular to the compression direction. Seismic fast axes for the mantle and crustal magnetic features therefore align, if vertically coherent deformation occurs in the region.

More recently, there have been suggestions of ancient subduction zones under the Slave Craton (Bostock, 1998; Davis et al., 2003), based on observations of converted and reflected seismic phases at mantle interfaces (e.g., Bostock, 1998). A seismic interface in the upper mantle under the Slave craton does seem to extent a long way to the west, and indeed all the way to the surface (Mercier et al., 2008). These studies have made the case for cratonic formation via shallow subduction processes (e.g., Vlaar, 1986; Abbott, 1991). There have been suggestions of ancient subduction events also for the Superior Province (e.g., Calvert et al., 1995). The observed correlation of mantle and crustal structure does not exclude such a model, since it is conceivable that the crust is deformed during such a subduction event. This would however give a clear constraint on the timing of the root-forming subduction event(s), which should be of neoarchean age (e.g., Davis et al., 2003).

An alternative to using magnetic data is the use of gravity anomalies. Those data are however less distance-sensitive, due to the $r^{-2}$-dependence of the gravitational field. The gravitational field is not only sensitive to (topography and) crustal structure, but also mantle structure, although the latter effect can be eliminated by high-pass filtering. Such an approach has been presented by Simons et al. (2003), however to a somewhat different problem. They have studied the correlation between topography and the Bouguer gravity anomaly to address a potential 'isostatic coherence anisotropy' that may give clues about 'mechanical anisotropy', and applied their technique to Australia. The technique presents an interesting theoretical approach, but it requires topography variations of which not much need to be left over in stable portions of continents. In contrast, the advantage of magnetic data is that they originate from the uppermost (crustal) portion only, and the clear correlation between crustal magnetics and mantle seismic anisotropy provides for a true comparison of independent quantities.

In order for our inferences to be correct, it is required that observed seismic anisotropy is not much perturbed by the crust. If this were the case, a correlation with crustal features would not be surprising. Some authors (Rümpker and Silver, 1998; Saltzer et al., 2002) have recently discussed whether there may be such a contamination by the crust. For that reason, we have performed numerical tests using an anisotropic two-layer case, and we have found that a potential crustal anisotropic layer has only minor effects on overall anisotropic parameters. For realistic anisotropic parameters for the crust the fast directions that are determined vary by just a few degrees, which is too weak to be detected.

Surface waves, receiver functions, and also backazimuthal variation of shear-wave splitting suggest that many regions around the world have (at least) two layers of anisotropy. Two such layers of anisotropy appear to be present also under the craton of North America (e.g., Bokelmann and Silver, 2000). Fast directions of the two layers appear to be rather similar though, and it may be difficult to distinguish them. This similarity is probably due to the fact that ancient fabric in crust and lithosphere is more or less parallel to absolute plate motion. More recently, non-zero dip angles of anisotropy for the bulk anisotropy have been interpreted as being due to the deeper anisotropic layer that may be due to plate-motion induced anisotropy (Bokelmann, 2002a,b). Other evidence for the existence of multiple layers in the Canadian shield have been provided by Kay et al. (1999), Bank and Bostock

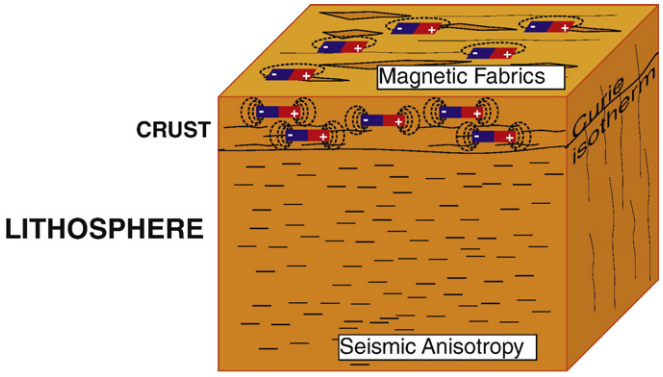


**Fig. 10.** Conceptual model explaining the similarity of crustal and mantle features on the craton. Both crust and mantle–lithosphere deform in transpression. Fabrics become perpendicular to the shortening direction, in both the crust and the mantle–lithosphere. These fabrics are apparent via magnetic lineaments in the crust, and seismic anisotropy in the mantle.

(2003), Snyder et al. (2003), and Musacchio et al. (2004). Beside shear-wave splitting, we have also compared magnetic fabric with anisotropic directions from surface waves, but we have not found much correlation. This is probably due to limited lateral resolution of the global surface wave models that we have used (e.g., Debayle et al., 2005), which is probably around thousand kilometers, but it may perhaps be better in some areas that are well-covered by seismic instrumentation (e.g., Wüstefeld et al., submitted for publication). The latter is not particularly the case for North American cratonic regions, and the tomographic models are apparently not yet capable of resolving inner-cratonic anisotropic structures. This may however change in the next few years with data from USArray becoming available for the stable portion of North America.

## 7. Conclusions

We have studied preferred orientation of fabric in crust and mantle for the stable portion of North America, using alignments of magnetic features in the crust, and seismic anisotropy for the upper mantle. Although totally independent, the two quantities show a remarkable correlation. This correlation is probably not fortuitous, and the best explanation is that the crust and mantle portions of the rather thick lithosphere of the North American Craton have been created together, and that at least 2.5 billion yr ago. In fact, the correlation is best where the lithosphere is the thickest, and the least perturbed by more recent tectonic activity.

Shear-wave splitting gives a relatively weak depth constraint, and it is often not clear whether the anisotropy is in the lithosphere or in the asthenosphere. The good correlation with crustal features indicates that much of the anisotropy observed above the shield is indeed in the lithosphere. A second anisotropic layer may not be easily distinguished in the stable portion of the North American plate. Indeed, absolute plate motion is quite close to this fast direction for the region under consideration.

The correlation between crustal magnetic features and mantle features also indicates that the 'magnetic' proxy for crustal fabric works well, at least in a transpressive deformation environment. Future studies of more tectonically active regions may perhaps reveal such a correlation for other tectonic settings. In fact, a global magnetic map compilation is available now (Purucker, 2007), and this kind of study can now be performed in various tectonic domains around the world.

## Acknowledgements

We wish to thank the many people who have helped to gather and assemble the magnetic map for North America. Robert Kucks helped with data conversion. Guilhem Barruol and Michael Bostock have read early versions of the manuscript. We thank Martha Savage and an anonymous reviewer for thoughtful reviews.

## References

Abbott, D., 1991. The case for accretion of the tectosphere by buoyant subduction. Geophys. Res. Lett. 18, 585–588.
Ando, M., Ishikawa, Y., 1982. Observations of shear-wave velocity polarization anisotropy beneath Honshu, Japan – 2 Masses with different polarizations in the upper mantle. J. Phys. Earth 30 (2), 191–199.
Ansel, V., Nataf, H-C., 1989. Anisotropy beneath 9 stations of the Geoscope broadband network as deduced from shear-wave splitting. Geophys. Res. Lett. 16, 409–412.
Babuska, V., Cara, M., 1991. Seismic Anisotropy in the Earth. Kluwer Academic Publishers, Dordrecht, the Netherlands.
Babuška, V., Plomerová, J., Šílený, J., 1984. Spatial variations of P residuals and deep structure of the European lithosphere. Geophys. J. R. Astron. Soc. 79, 363–383.
Bank, C.-G., Bostock, M.G., 2003. Linearized inverse scattering of teleseismic waves for anisotropic crust and upper mantle structure: 2. Numerical examples and applications to data from Canadian stations. J. Geophys. Res. 108, B5. doi:10.1029/2002JB001950.
Bank, C.-G., Bostock, M.G., Ellis, R.M., Cassidy, J.F., 2000. A reconnaissance teleseismic study of the upper mantle and transition zone beneath the Archean Slave craton in NW Canada. Tectonophysics 319 (3), 151–166.
Bankey, V., Cuevas, A., Daniels, D., Finn, C.A., Hernandez, I., Hill, P., Kucks, R., Miles, W., Pilkington, M., Roberts, C., Roest, W., Rystrom, V., Shearer, S., Snyder, S., Sweeney, R., Velez, J., Phillips, J., Ravat, D.K.A., 2002. Digital data grids for the magnetic anomaly map of North America. USGS Open-File Report 02-414.
Barruol, G., Mainprice, D., 1993. A quantitative evaluation of the contribution of crustal rocks to the shear wave splitting of teleseismic SKS waves. Phys. Earth Planet. Inter. 78, 281–300.
Barruol, G., Silver, P.G., Vauchez, A., 1997. Seismic anisotropy in the eastern US: Deep structure of a complex continental plate. J. Geophys. Res. 102 (B4), 8329–8348.
Barruol, G., Souriau, A., Vauchez, A., Diaz, J., Gallart, J., Tubia, J., Cuevas, J., 1998. Lithospheric anisotropy beneath the Pyrenees from shear wave splitting. J. Geophys. Res. 103 (B12), 30039–30053.
Bokelmann, G.H.R., 1995. P-wave array polarization analysis and effective anisotropy of the brittle crust. Geophys. J. Int. 120 (1), 145–162.
Bokelmann, G.H.R., 2002a. Convection-driven motion of the North American craton: evidence from P-wave anisotropy. Geophys. J. Int. 248 (2), 278–287.
Bokelmann, G.H.R., 2002b. Which forces drive North America? Geology 30 (11), 1027–1030.
Bokelmann, G.H.R., Silver, P.G., 2000. Mantle variation within the Canadian Shield: travel times from the APT89 portable broadband transect. J. Geophys. Res. 105, 579–605.
Bokelmann, G.H.R., Silver, P.G., 2002. Shear stress at the base of shield lithosphere. Geophys. Res. Lett. 29 (23), 2091. doi:10.1029/2002GL015925.
Bormann, P., Burghardt, P., Makeyeva, L.I., Vinnik, L.P., 1993. Teleseismic shear-wave splitting and deformations in Central Europe. Phys. Earth Planet. Inter. 78, 157–166.
Bostock, M.G., 1998. Mantle stratigraphy and evolution of the Slave craton. J. Geophys. Res. 103 (B9), 21183–21200.
Bowman, J.R., Ando, M., 1987. Shear-wave splitting in the upper-mantle wedge above the Tonga subduction zone. Geophys. J. R. Astron. Soc. 88, 25–41.
Calvert, A.J., Sawyer, E.W., Davis, W.J., Ludden, J.N., 1995. Archaean subduction inferred from seismic images of a mantle suture in the Superior Province. Nature 375, 670–674.
Card, K.D., 1990. A review of the Superior Province of the Canadian shield, a product of Archean accretion. Precambrian Res. 48, 99–156.
Chiozzi, P., Matsushima, J., Okubo, Y., Pasquale, V., Verdoya, M., 2005. Curie-point depth from spectral analysis of magnetic data in central-southern Europe. Phys. Earth Planet. Inter. 152, 267–276.
Davis, W.J., Jones, A.G., Bleeker, W., Grütter, H., 2003. Lithosphere development in the Slave craton: a linked crustal and mantle perspective. Lithos 71, 575–589.
Debayle, E., Kennett, B., Priestley, K., 2005. Global azimuthal seismic anisotropy and the unique plate motion of Australia. Nature 433, 509–512.
Eaton, D.W., Jones, A.G., Ferguson, I.J., 2004. Lithospheric anisotropy structure inferred from collocated teleseismic and magnetotelluric observations: Great Slave Lake shear zone, northern Canada. Geophys. Res. Lett. 31, L19614. doi:10.1029/2004GL020939.
Ernst, R.E., Grosfils, E.B., Mège, D., 2001. Giant dike swarms: Earth, Venus, and Mars. Annu. Rev. Earth Planet. Sci. 29, 489–534. doi:10.1146/annurev.earth.29.1.489.
Fouch, M.J., Rondenay, S., 2006. Seismic anisotropy beneath stable continental interiors. Phys. Earth Planet. Int. 158 (2–4), 292–320.
Fouch, M.J., Fischer, K.M., Parmentier, E.M., Wysession, M.E., Clarke, T.J., 2000. Shear wave splitting, continental keels, and patterns of mantle flow. J. Geophys. Res. 105 (B3), 6255–6275.
Fukao, Y., 1984. Evidence from core-reflected shear waves for anisotropy in the Earth's mantle. Nature 309 (5970), 695–698.
Frederiksen, A., Ferguson, I., Eaton, D., Miong, S.-K., Gowan, E., 2006. Mantle fabric at multiple scales across an Archean-Proterozoic boundary, eastern Ontario, Canada. Phys. Earth Planet. Inter. 158, 240–263.
Gilder, S.A., LeGoff, M., Peyronneau, J., Chervin, J.-C., 2002. Novel high pressure magnetic measurements with application to magnetite. Geophys. Res. Lett. 29, 10. doi:10.1029/2002GL014227.
Grand, S.P., 1994. Mantle shear structure beneath the Americas and surrounding oceans. J. Geophys. Res. 99, 11591–11621.
Hansen, R.O., de Ridder, E., 2006. Linear feature analysis for aeromagnetic data. Geophysics 71 (6), L61–L67.
Heintz, M., Kennett, B.L.N., 2006. The apparently isotropic Australian upper mantle. Geophys. Res. Lett. 33, L15319.
Hoffman, P.F., 1989. Precambrian geology and tectonic history of North America. In: Bally, A.W., Palmer, A.R. (Eds.), The Geology of North America—An Overview. Geological Society of America. Boulder, pp. 447–511.
Hoffman, P.F., 1990. Geological constraints on the origin of the mantle root beneath the Canadian Shield. Philos. Trans. R. Soc. Lond. 331, 523–532.
James, D.E., Assumpcao, M., 1996. Tectonic implications of S-wave anisotropy beneath SE Brazil. Geophys. J. Int. 126 (1), 1–10.
Ji, S.C., Rondenay, S., Mareschal, M., Senechal, G., 1996. Obliquity between seismic and electrical anisotropies as a potential indicator of movement sense for ductile shear zones in the upper mantle. Geology 24 (11), 1033–1036.
Jordan, 1975. The continental tectosphere. Rev. Geophys. 13, 1–12.
Jordan, 1978. Composition and development of continental tectosphere. Nature 274, 544–548.
Jordan, T.H., 1988. Structure and formation of continental tectosphere. J. Petrol. 11–37.
Karato, S.I., Wu, P., 1993. Rheology of the upper mantle: a synthesis. Science 260, 771–778.
Kay, I., Sol, S., Kendall, J-M., Thomson, C., White, D., Asudeh, I., Roberts, B., Francis, D., 1999. Shear wave splitting observations in the Archean craton of Western Superior. Geophys. Res. Lett. 26, 2669–2672.
LeCheminant, A.N., 1994. Proterozoic diabase dyke swarms, Lac de Gras and Aylmer Lake area, District of Mackenzie, Northwest Territories. Geological Survey of Canada, Open File 2975, scale 1:250 000.

Mainprice, D., Silver, P.G., 1993. Interpretation of SKS-waves using samples from the subcontinental lithosphere. Phys. Earth Planet. Int. 78, 257–280.
Mainprice, D., Barruol, G., Ben Ismail, W., 2000. The seismic anisotropy of the Earth's mantle: from single crystal to polycrystal. In: Karato, S.I. (Ed.), Earth's Deep Interior: Mineral Physics and Tomography from the Atomic to the Global Scale. . Geodyn. Ser. AGU, Washington, D.C., pp. 237–264.
Maus, S., Rother, M., Holme, R., Luhr, H., Olsen, N., Haak, V., 2002. First scalar magnetic anomaly map from CHAMP satellite data indicates weak lithospheric field. Geophys. Res. Lett. 29. doi:10.1029/2001GL013685.
McKenzie, D., 1979. Finite deformation during fluid flow. Geophys. J. Int. 58 (3), 689–715.
Mercier, J.-P., Bostock, M.G., Audet, P., Gaherty, J.B., Garnero, E.J., Revenaugh, J., 2008. The teleseismic signature of fossil subduction: Northwestern Canada. J. Geophys. Res. 113, B04308. doi:10.1029/2007JB005127.
Montagner, J., 1986. Three-dimensional structure of the Indian ocean inferred from long-period surface waves. Geophys. Res. Lett. 13, 315–318.
Musacchio, G., White, D.J., Asudeh, I., Thomson, C.J., 2004. Lithospheric structure and composition of the Archean western Superior Province from seismic refraction/wide-angle reflection and gravity modeling. J. Geophys. Res. 109, B03304.
Neidell, N.S., Taner, M.T., 1971, Semblance and other coherency measures for multi-channel. data: Geophysics, Soc. Explor. Geophys., 36, 482–497.
Nicolas, A., Christensen, N.I., 1987. Formation of anisotropy in upper mantle peridotites — A review. In: Fuchs, K., Froideveaux, C. (Eds.), Composition Structure and Dynamics of the Lithosphere Asthenosphere System. AGU, Washington D.C., pp. 111–123.
Nicolas, A., Boudier, F., Boullier, A.M., 1973. Mechanisms of flow in naturally and experimentally deformed peridotites. Am. J. Sci. 273, 853–876.
Pilkington, M., Roest, W.R., 1998. Removing varying directional trends in aeromagnetic data. Geophysics 63, 446–453.
Purucker, M.E., 2007. Magnetic anomaly map of the world. EOS 88, 25, 263.
Raitt, R.W., Shor, G.G., Francis, T.J.G., Morris, G.B., 1969. Anisotropy of Pacific upper mantle. J. Geophys. Res. 74 (12), 3095–3109.
Rondenay, S., Bostock, M.G., Hearn, T.M., White, D.J., Ellis, R.M., 2000a. Lithospheric assembly and modification of the SE Canadian Shield: Abitibi-Grenville teleseismic experiment. J. Geophys. Res. 105, 13,735–13,754.
Rondenay, S., Bostock, M.G., Hearn, T.M., White, D.J., Wu, H., Sénéchal, G., Ji, S., Mareschal, M., 2000b. Teleseismic studies of the lithosphere below the Lithoprobe Abitibi-Grenville Transect. Can. J. Earth Sci. 37, 415–426.
Rümpker, G., Silver, P.G., 1998. Apparent shear-wave splitting parameters in the presence of vertically-varying anisotropy. Geophys J. Int. 135, 790–800.
Saltzer, R.L., Gaherty, J.B., Jordan, T.H., 2002. How are vertical shear wave splitting measurements affected by variations in the orientation of azimuthal anisotropy with depth? Geophys. J. Int. 141 (2), 374–390.
Samara, G.A., Giardini, A.A., 1969. Effect of pressure on the Néel temperature of magnetite. Phys. Rev. 186 (2), 577–580.
Savage, M.K., 1999. Seismic anisotropy and mantle deformation: what have we learned from shear wave splitting. Rev. Geophys. 37, 69–106.
Schult, A., 1970. Effect of pressure on the Curie temperature of titanomagnetites [(1−x) Fe3O4−x TiFe2O4]. Earth Planet. Sci. Lett. 10 (1), 81–85.
Schulte-Pelkum, V., Blackman, D.K., 2003. A synthesis of seismic P and S waves. Geophys. J. Int. 154 (1), 166–178.
Schulte-Pelkum, V., Masters, G., Shearer, P.M., 2001. Upper mantle anisotropy from long-period P polarization. J. Geophys. Res. 106, 21917–21934.
Sénéchal, G., Rondenay, S., Marechal, M., Guilbert, J., Poupinet, G., 1996. Seismic and electrical anisotropies in the lithosphere across the Grenville Front. Geophys. Res. Lett. 23, 2255–2258.
Sieminski, A., Liu, Q., Trampert, J., Tromp, J., 2007. Finite-frequency sensitivity of body waves to anisotropy based upon adjoint methods. Geophys. J. Int. 171, 368–389.
Silver, P.G., 1996. Seismic anisotropy beneath the continents: probing the depths of geology. Annu. Rev. Earth Planet. Sci. 24, 385–432.
Silver, P.G., Chan, W.W., 1988. Implications for continental structure and evolution from seismic anisotropy. Nature 335, 34–39.
Silver, P.G., Chan, W.W., 1991. Shear wave splitting and subcontinental mantle deformation. J. Geophys. Res. 96 (B10), 16429–16454.
Silver, P.G., Kaneshima, S., 1993. Constraints on mantle anisotropy beneath Precambrian North America from a transportable teleseimic experiment. Geophys. Res. Lett. 20, 1127–1130.
Silver, P.G., Savage, M., 1994. The interpretation of shear-wave splitting parameters in the presence of two anisotropic layers. Geophys. J. Int. 119, 949–963.
Silver, P.G., Mainprice, D., Ben Ismaïl, W., Tommasi, A., Barruol, G., 1999. Mantle structural geology from seismic anisotropy. In: Fei, Y., Bertka, C.M., Mysen, B.O. (Eds.), Mantle Petrology : Field Observations and High Pressure Experimentation: A Tribute to Francis R. (Joe) Boyd. The Geochemical Society Special Publication, 6, pp. 79–103.
Simons, F.J., van der Hilst, R.D., Zuber, M.T., 2003. Spatiospectral localization of isostatic coherence anisotropy in Australia and its relation to seismic anisotropy: Implications for lithospheric deformation. J. Geophys. Res. 108 (B5). doi:10.1029/2001JB000704.
Snyder, D.B., Bostock, M.G., Lockhart, G.D., 2003. Two anisotropic layers in the Slave craton. Lithos 71 (2–4), 529–539. doi:10.1016/j.lithos.2003.09.001.
Teyssier, C., Tikoff, B., Markley, A., 1995. Oblique plate motion and continental tectonics. Geology 23 (5), 447–450.
Tikoff, B., Russo, R., Teyssier, C., Tommasi, A., 2004. Mantle-driven deformation of orogenic zones and clutch tectonics. In: Grocott, J., McCaffrey, K.J.W., Taylor, G., Tikoff, B. (Eds.), Vertical Coupling and Decoupling in the Lithosphere. Geol. Soc. Spec. Publ., 227, pp. 41–64.
Vauchez, A., Nicolas, A., 1991. Mountain building: strike parallel motion and mantle anisotropy. Tectonophysics 185, 183–201.
Vinnik, L.P., Kosarev, G.L., Makeyeva, L.I., 1984. Anisotropiya litosfery po nablyudeniyam voln SKS and SKKS'. Dokl. Akad. Nauk USSR 278, 1335–1339.
Vinnik, L.P., Makeyeva, L.I., Milev, A., Usenko, Y., 1992. Global patterns of azimuthal anisotropy and deformation in the continental mantle. Geoph. J. Int. 111, 433–447.
Vlaar, N.J., 1986. Archean global dynamics. Geology 65, 91–101.
Wüstefeld, A., Bokelmann, G.H.R., Zaroli, C., Barruol, G., 2008. SplitLab: a shear-wave splitting environment in Matlab. Comput. Geosci. 34, 515–528. doi:10.1016/j.cageo.2007.08.002.
Wüstefeld, A., Bokelmann, G.H.R., Barruol, G., Montagner, J.P., submitted for publication, Correlation of global seismic anisotropy from SKS splitting and surface waves, EPSL.
Zhang, L., Wu, J., Hao, T., Wang, J., 2006. Automatic lineament extraction from potential-field images using the Radon transform and gradient calculation. Geophysics 71 (3), J31–J40.